Indian Journal of
Applied Radiology

Open Science Publications

Volume 12, Issue 1 - 2026
© Kumar K, et al. 2026
www.opensciencepublications.com

Computed Tomography Cerebral Angiography Evaluation of Cerebral Arterial Aneurysms-Case Series

Case Report

Kumar K*, Raveendran C, Murugaiah V and Senthilnathan V

Department of Radio-diagnosis. Trichy SRM Medical College Hospital and Research Centre. Irungalur, Trichy, Tamil Nadu, India

***Corresponding author:** Krishna Kumar M, Department of Radio-diagnosis. Trichy SRM Medical College Hospital and Research Centre. Irungalur, Trichy, Tamil Nadu, India. E-mail Id: drmkrishnakumar@gmail.com

Copyright: © 2026 Kumar K, et al. This is an open access article distributed under the Creative Commons Attribution License, which permits unrestricted use, distribution, and reproduction in any medium, provided the original work is properly cited.

Article Information: **Submission: 07/01/2026; Accepted: 15/04/2026; Published: 18/04/2026**

Abstract

Objective: Saccular (berry-shaped) aneurysms that develop at arterial bifurcations—branch points where an artery splits into two branches—are the most common type of intracranial aneurysms, which are aberrant focal dilatations (localized bulges) of cerebral arteries. When they burst, cerebral artery aneurysms (CAA) pose a serious risk of morbidity and death. This case series aims to analyze computed tomography cerebral angiography (CTCA), a medical imaging method for the screening, diagnosis, and follow-up of patients with cerebral artery aneurysms that uses CT scans to show cerebral arteries.

Conclusion: Recent years have seen a significant change in the diagnosis and treatment of cerebral aneurysms. With CTCA, radiologists can accurately describe pertinent results, such as the risk of aneurysm rupture, and reliably and noninvasively identify the majority of intracranial aneurysms. Additionally, it helps identify high-risk groups and recommend screening. Treatment is becoming safer and more efficient thanks to nonoperative endovascular treatments, which are minimally invasive operations carried out inside blood vessels..

Keywords: Subarachnoid Hemorrhage; Fusiform Aneurysm; Dolichoectasia; Bilobed Aneurysm; Mycotic Aneurysm; Giant Aneurysm; Computed Tomography Cerebral Angiography

Introduction

Although the majority of cerebral artery aneurysms [CAA] may not cause any symptoms over a patient's lifetime, ruptures can have disastrous consequences. About 80–90% of non-traumatic subarachnoid hemorrhages (SAH) are caused by them (Figures 1A, 2A, 2B, 3A, 4A, 4B, 5A, 5B, 6A, 6B, and 7A). Position, size, high-danger characteristics (irregular protrusions and/or daughter sacs), patient characteristics (age, gender, race), and extra risk factors (hypertension, prior SAH, smoking) all influence the rupture hazard of CAA [1]. Saccular (berry) aneurysms are the most common type of intracranial aneurysms, and they are found in predictable locations around the circle of Willis. However, uncommon aneurysm types can occasionally be found, such as dissecting, fusiform, serpentine, blood blister type, traumatic, mycotic (or infectious), atheromatous, and enormous aneurysms, all of which can cause focal bleeding (Figure. 1A, Figure 8A, 9A), thromboembolic episodes, or bulk effect [2] (Figure. 10A). Conventional neurovascular imaging techniques such as CTCA, magnetic resonance angiography (MRA), and digital subtraction angiography (DSA) can be used to assess CAA, morphologic features, and post-treatment appearance. The diagnostic accuracy of noninvasive imaging for initial opinion and surveillance has improved with to advancements in computed tomography and CTCA, transcranial Doppler sonography, and MRA, even if DSA is still the

ISSN: 2581-3919

gold standard for CAA characterisation and treatment planning. Hospitalization for aneurysmal subarachnoid hemorrhage decreased slightly but significantly with increased use of neuroimaging and treatment of unruptured CAA.

We examine the CTCA imaging methods and manifestations of CAA in this patient population's assessment, monitoring, management, and results.

Discussion

Approximately 4% of people have intracranial aneurysms, making them fairly common. The majority of these aneurysms are asymptomatic, but they do present a slight but real risk of rupturing and causing acute SAH [3].

The internal elastic lamina and a weakened or absent muscularis layer are typically the two layers of the normal artery wall that are lacking in all real cerebral aneurysms. All layers of the artery wall are lacking in intracranial pseudoaneurysms, which are typically cavitated paravascular hematomas that may or may not connect directly with the real arterial lumen. The "blood blister-like" aneurysm is uncommon yet deadly because of its tissue-paper thin wall. Round or lobulated focal outpouchings known as saccular aneurysms typically develop at major artery bifurcations, which are regions of severe hemodynamic stress [3].

In the arteries of the circle of Willis, saccular aneurysms usually affect the following arteries in order of frequency [4]. The middle cerebral artery (20%) (Figure1, Figure 2, Figure 9, Figure 13, Figure 24), the anterior communicating artery (30%) (Figure 3, Figure 4, Figure 7, Figure 10, Figure 11, Figure 12, Figure 23), the internal carotid artery (8%) (Figure 6, Figure 13, Figure 14, Figure 15, Figure 16, Figure 17, Figure 18, Figure 20), and the tip of the basilar artery (Figure 21), Pericallosal anterior cerebral artery (4%) (Figure 8, 12) and posterior inferior cerebellar artery (3%). Fusiform aneurysms (Dolichoectasia) (Figure 25) are long, spindle-shaped arterial dilations that may be linked to non-atherosclerotic pathology, such as connective tissue disorders, or atherosclerotic vascular disease [3]. Ectatic sinuous cerebral arteries, which are most commonly found in the vertebrobasilar system, give rise to dolicoectasia, which can have a diameter of several centimeters. Although symptoms of brainstem or cranial-nerve compression are typically present in these situations, they are not typically linked to SAH [5]. A ruptured artery or cystic medial necrosis are the causes of dissecting aneurysms. Thirty percent of affected people develop multiple aneurysms [5] - According to the Unruptured Cerebral Aneurysm Study [6], aneurysms should be classified as small (<5 mm), medium (>5-10 mm), large (>10 mm-25 mm), and giant (>25 mm) based on the maximum dome diameter. A neck diameter greater than 4 mm or a dome-to-neck ratio less than 2 were indicative of a wide-neck aneurysm.

Giant fusiform aneurysms are thought to be less common than 1% of all intracranial aneurysms, while "giant aneurysms"-intracranial aneurysms with a diameter more than 25 mm-represent between 3-5% of all aneurysms. A gigantic aneurysm presentation is characterized by the presence of a mural thrombus, cerebral bleeding episodes, and expansion symptoms [7].

Case 1: A 70-year-old woman was referred for CTCA after experiencing an abrupt, intense headache, eye pain, and weakness and numbness on her right side. She had a history of hypertension and inconsistent therapy.

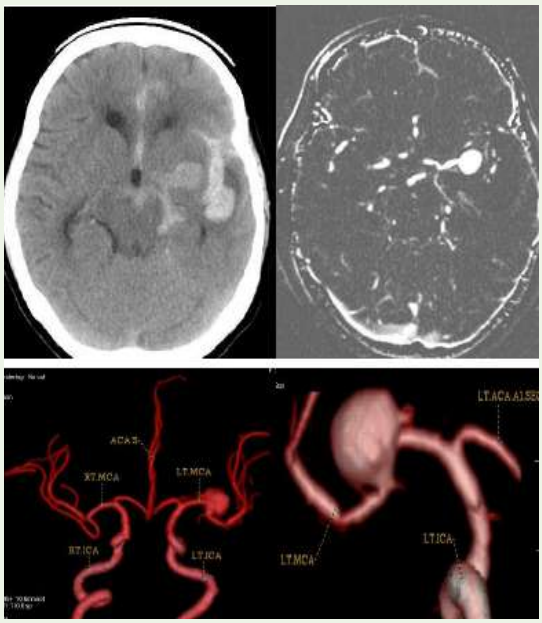

Figure 1: Acute SAH is visible along the anterior interhemispheric fissure, left sylvian fissure, interpeduncular cistern, left ambient cistern, and left basal ganglia hemorrhage on noncontrast CT (A). A significant saccular aneurysm is visible at the left middle cerebral artery (MCA) bifurcation in CTCA maximum intensity projection (MIP) (B) and 3D volume rendered images (3D-VR) (C, D). She received medical care and was recommended for endovascular coiling or surgical clipping.

Case 2: A 60-year-old woman was referred for CTCA due to a persistent headache, meningeal symptoms, and neurological impairment. She was taking medicine for both hypertension and type 2 diabetes.

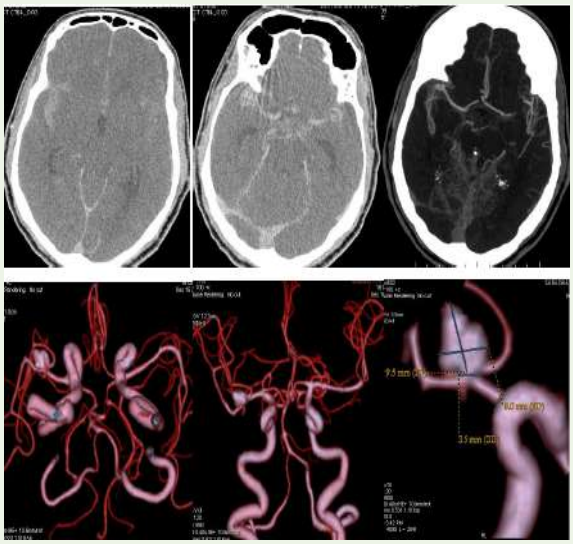

Figure 2: Acute SAH is visible in basal cisterns, sylvian fissures, interhemispheric fissures, and along the tentorium cerebelli on noncontrast CT (A, B). A medium multilobed Saccular aneurysm measuring 9.5x6 mm with a neck diameter of 3.5 mm is shown at the right MCA bifurcation in CTCA (C) and 3D-VR images (D, E, and F). She had conservative care and was recommended for endovascular therapy and /or surgical clipping.

Citation: Kumar K, Raveendran C, Murugaiah V, Senthilnathan V. Computed Tomography Cerebral Angiography Evaluation of Cerebral Arterial Aneurysms-Case Series. Indian J Appl Radiol. 2026;12(1): 231.

Case 3: A 65-year-old woman receiving therapy for hypertension is referred for CTCA after experiencing seizures and loss of consciousness.

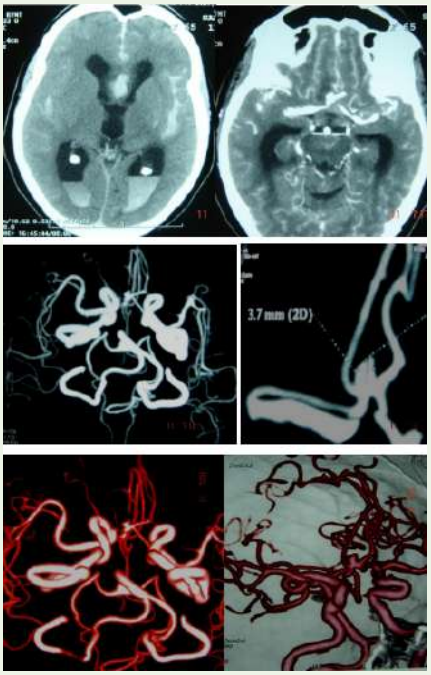

Figure 3: Noncontract CT (A) reveals intraventricular hemorrhage in the posterior horns of lateral ventricles as well as acute SAH in Sylvian fissures, interhemispheric fissures, and along cerebral sulci. Anterior communicating artery (ACOM) saccular aneurysm is visible on CTCA (B), MIP (C, D), and 3D-VR (E, F) images. During conservative treatment, the patient passed away.

Case 4: A 48-year-old man who smokes regularly and has a severe headache was sent for CTCA.

Figure 4: Acute SAH is visible at the tentorium cerebelli and cerebral sulci interhemispheric fissure on noncontrast CT (A, B). Multilobed medium ACOM saccular aneurysms measuring 10.8x7.6 mm and left MCA bifurcation small saccular aneurysms measuring 6.1x4.9 mm are visible in CTCA axial (C, D) and 3D-VR images (E–H). He received conservative care and did not return for a follow-up.

Case 5: A 62-year-old man with a history of hypertension who presents with severe headaches, nausea, and vomiting is referred for CTCA

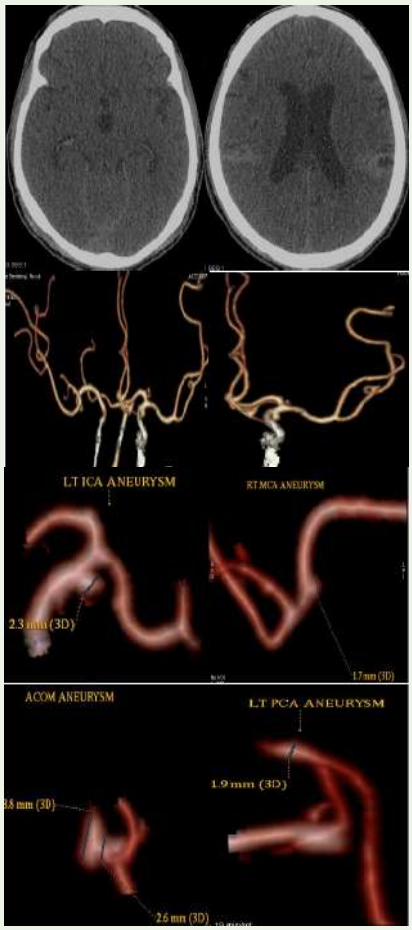

Figure 5: Acute SAH is seen on noncontrast CT (A, B). Multiple saccular aneurysms of intracranial left clinoid ICA (C5), ACOM, right MCA, and fusiform aneurysm of left posterior cerebral artery (PCA) are seen on CTCA 3D-VR images (C-H). Managed conservatively & on regular follow up.

Case 6: A 50-year-old man with a severe “thunderclap” headache and left double vision was referred for CTCA due to his longstanding alcoholism.

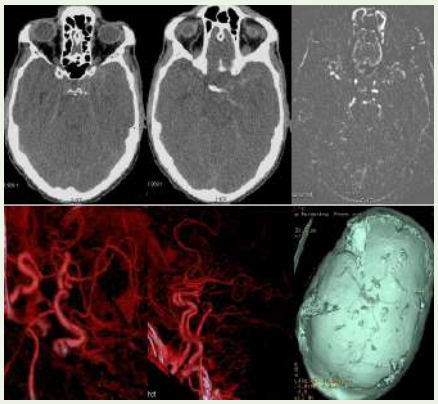

Figure 6: (A-F). Acute SAH is visible along the left parasellar cistern, suprasellar cistern, and tentorium cerebelli on noncontrast CT (A, B). The left intracavernous ICA (C4) saccular aneurysm is seen in CTCA MIP (C) and 3D-VR pictures (D-F). Endovascular therapy was recommended for him.

Citation: Kumar K, Raveendran C, Murugaiah V, Senthilnathan V. Computed Tomography Cerebral Angiography Evaluation of Cerebral Arterial Aneurysms-Case Series. Indian J Appl Radiol. 2026;12(1): 231.

Case 7: A 63-year-old man with a severe headache and inconsistent hypertension therapy was referred for CTCA.

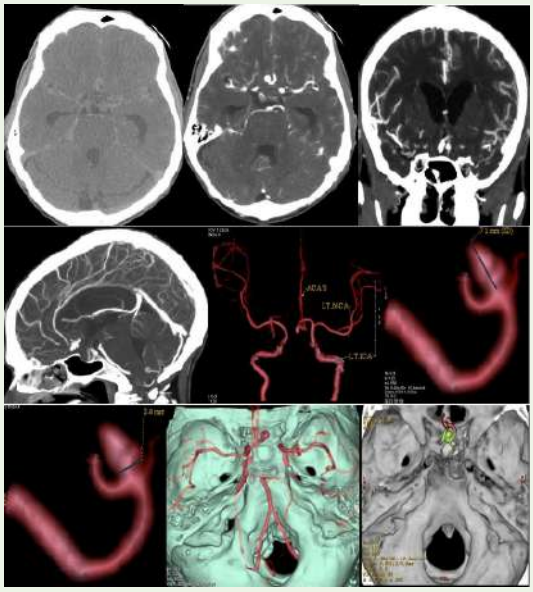

Figure 7: Noncontrast CT (A), shows acute SAH. A medium saccular aneurysm of ACOM with a neck diameter of 3.4 mm is visible on CTCA (B-D), 3D-VR pictures (E-G), and 3D-VR virtual dissection (H, I).
Endovascular coiling and/or surgical clipping were recommended for him.

Case 8: A 70-year-old male patient receiving therapy for Type 2 diabetes mellitus and hypertension presented with abrupt left hemiparesis and altered sensorium, which were examined by CTCA.

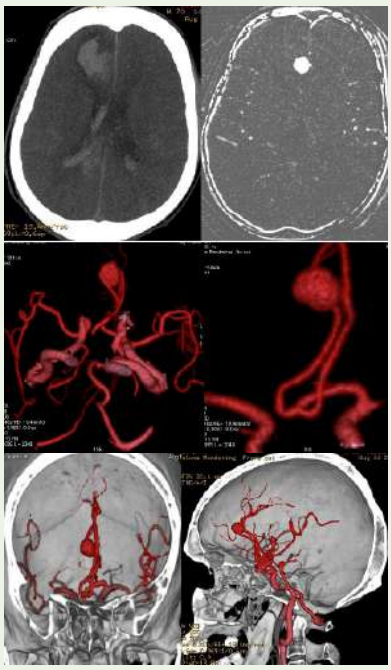

Figure 8: Noncontrast axial (A) show Right frontal lobe lobulated hematoma with surrounding edema, acute SAH and intraventricular hemorrhage, MIP (B), 3D-VR (C, D), and virtual dissection of skull images (E, F) all show a large right precallosal ACA (A3) saccular aneurysm projecting to the right. He received conservative treatment and advised endovascular coiling and/or surgical clipping, and frequent follow-up.

Case 9: A 65-year-old man was referred for CTCA after exhibiting abrupt onset of a left focal neurological impairment and impaired sensorium.

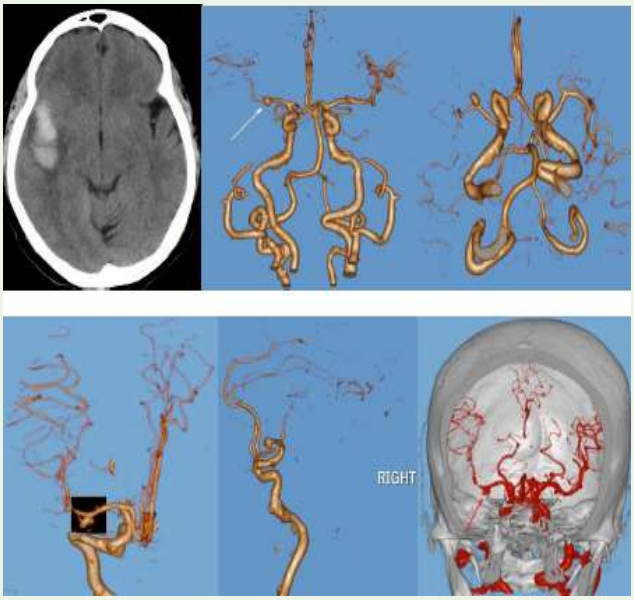

Figure 9: Right temporal lobe lobulated hematoma with surrounding edema is visible on CT axial non-contrast (A), whereas right MCA (M1) saccular aneurysm projecting inferiorly is visible on 3D-VR (B-E) and virtual dissection (F) images. Treated consevatively & on regular follow up.

Case 10: A 43-year-old woman was referred for CTCA after exhibiting sensory loss and weakness in her left leg.

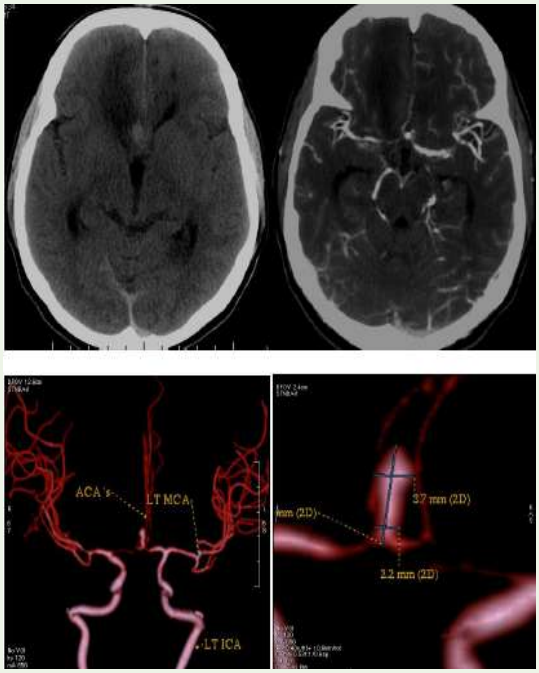

Figure 10: Right frontal lobe infarct is seen on CT Axial non-contrast (A), MIP (B), and 3D-VR images (C, D) show a large ACOM saccular aneurysm with a neck diameter of 2.2 mm and a high ellipticity index, squeezing the right ACA's A2 segment and generating a mass effect. He was scheduled for immediate endovascular treatment but did not show up for the follow-up.

Citation: Kumar K, Raveendran C, Murugaiah V, Senthilnathan V. Computed Tomography Cerebral Angiography Evaluation of Cerebral Arterial Aneurysms-Case Series. Indian J Appl Radiol. 2026;12(1): 231.

Case 11: A 63-Year-Old Man Smoker Who Is Recommended for CTCA Due To Persistent Headaches.

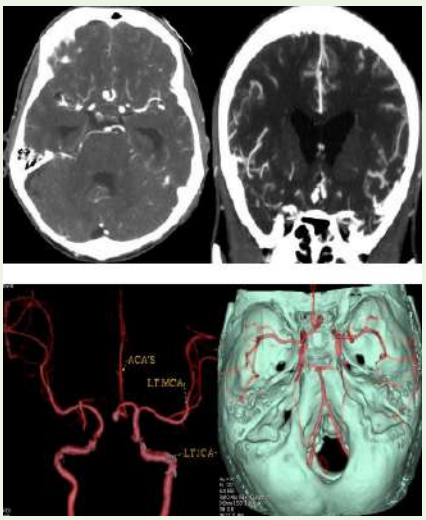

Figure 11: ACOM saccular aneurysm extending anteriorly is seen in CTCA axial (A), coronal (B), 3D-VR (C), and virtual dissection of skull vault pictures (D). He is routinely monitored.

Case 12: A 75-Year-Old Man Receiving Medication for Hypertension Was Referred for CTCA Due To a Recurrent Headache..

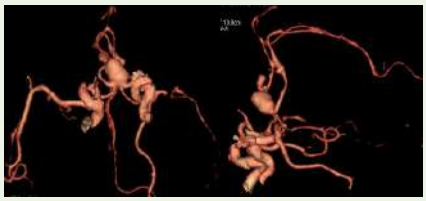

Figure 12: Large saccular aneurysms of ACOM and smaller saccular aneurysms of bilateral A2 segments of ACA are shown in CTCA 3D-VR pictures. He is being monitored on a regular basis.

Case 13: CTCA 3D-VR pictures show a small left MCA bifurcation saccular aneurysm measuring 3.2x2.9 mm and a large left ICA bifurcation multilobed saccular aneurysm with bleb measuring 10.2x9.4 mm and neck diameter of 7.1 mm. Endovascular therapy was scheduled for him.

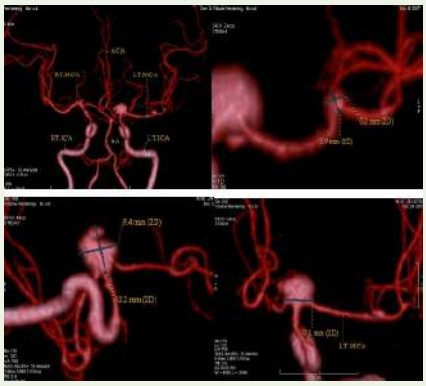

Figure 13: CTCA 3D-VR pictures show a small left MCA bifurcation saccular aneurysm measuring 3.2x2.9 mm and a large left ICA bifurcation multilobed saccular aneurysm with bleb measuring 10.2x9.4 mm and neck diameter of 7.1 mm. Endovascular therapy was scheduled for him.

Case 14: A 65-year-old woman on diabetes medication reports having frequent headaches; CTCA is recommended.

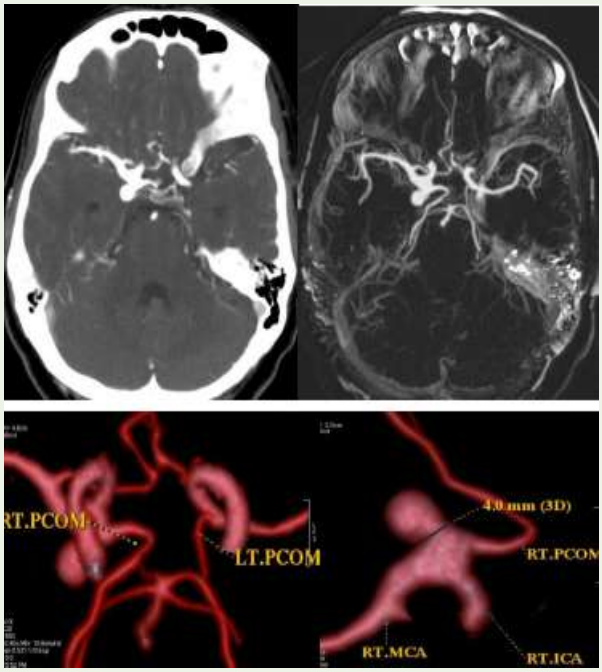

Figure 14: CTCA Axial (A), MIP (B), and 3D-VR images (C, D) show a medium saccular aneurysm with a neck diameter of 4 mm at the intersection of the right ICA bifurcation and the origin of the posterior communicating artery (PCOM). Endovascular therapy and follow-up were recommended for her.

Case 15: A 60-year-old woman with a history of persistent, recurrent headaches is advised to undergo CTCA.

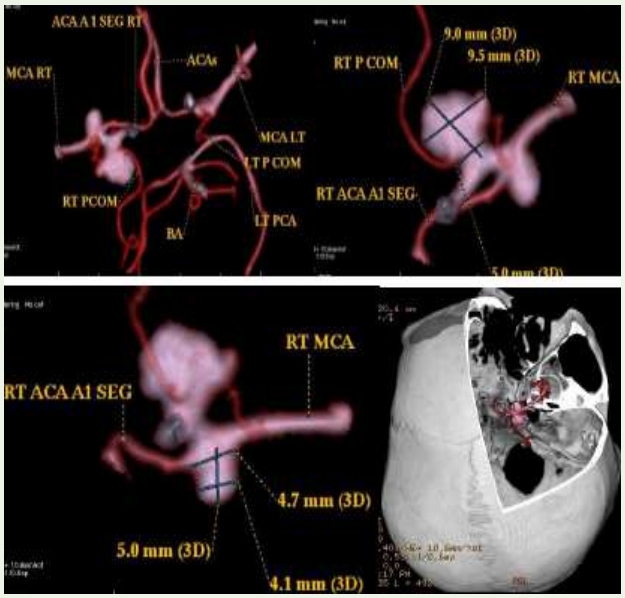

Figure 15: CTCA 3D-VR pictures (A–C) and virtual dissected skull bone (D) show a small saccular aneurysm with a neck diameter of 4.7 mm that originates from the right ICA bifurcation and measures 5 x 4.1 mm. Another medium multilobed saccular aneurysm, measuring 9.5 x 9 mm with a neck diameter of 5 mm, originated at the intersection of the right PCOM and MCA. Endovascular therapy and further monitoring were recommended for her.

Citation: Kumar K, Raveendran C, Murugaiah V, Senthilnathan V. Computed Tomography Cerebral Angiography Evaluation of Cerebral Arterial Aneurysms-Case Series. Indian J Appl Radiol. 2026;12(1): 231.

Case 16: A 62-year-old man with uncontrolled hypertension who complained of frequent headaches had CTCA.

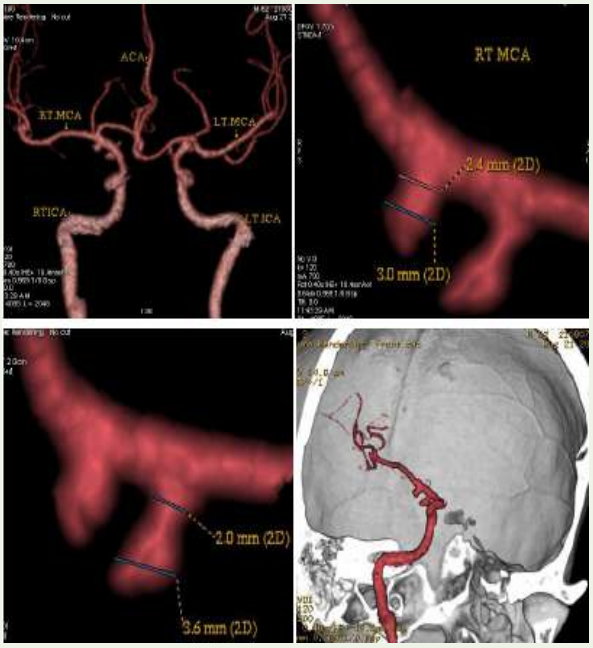

Figure 16: Two medium saccular aneurysms with a high ellipticity index in the right distal communicating ICA (C7) with neck diameters of 2 mm and 2.4 mm, respectively, are seen in CTCA 3D-VR (A-C) and virtual dissected skull vault (D) pictures. Endovascular therapy was recommended for him.

Case 17: A 55-year-old woman with a persistent headache and a history of SAH underwent CTCA.

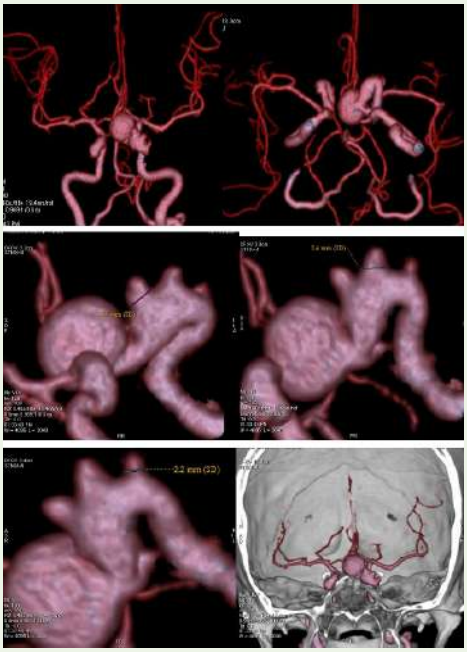

Figure 17: Left ICA bifurcation large saccular aneurysm and three small saccular aneurysms of terminal communicating ICA (C7) with neck diameters of 3.7 mm, 3.6 mm, and 2.2 mm are visible in CTCA 3D-VR (A-E) and virtual dissection of skull (F) pictures. Endovascular therapy and follow-up were recommended for her.

Case 18: A 64-year-old man was referred for CTCA due to a persistent headache and blurred vision in his left eye.

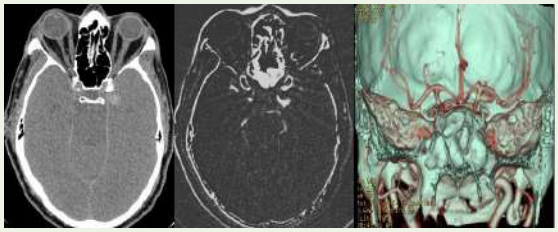

Figure 18: CT Noncontrast axial (A), CTCA MIP (B), and virtual dissection of the skull (C) images show a left supraclinoid ophthalmic ICA (C6) small saccular aneurysm. Endovascular therapy and routine follow-up were recommended for him.

Case 19: A 45-year-old man with bilateral impaired vision and a persistent, severe headache was referred for CTCA.

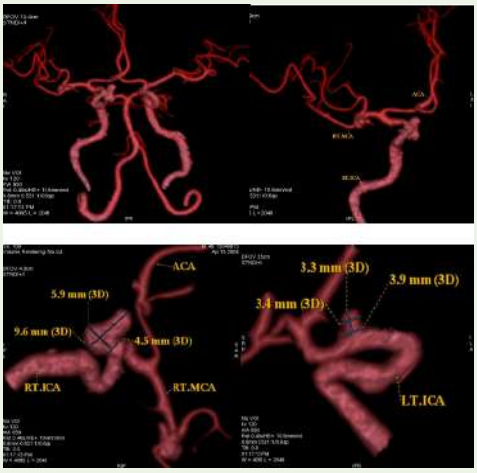

Figure 19: Bilateral distal ophthalmic ICA(C6) saccular aneurysms measuring right medium 9.6x5.9 mm with neck diameter of 4.5 mm and left small 3.3x3.4 mm with neck diameter of 3.9 mm are shown on CTCA 3D-VR (A-D) images. Endovascular treatment was recommended for him, but he did not show up for the follow-up.

Case 20: A 35-year-old man was referred for CTCA due to a persistent headache that was being treated with analgesics.

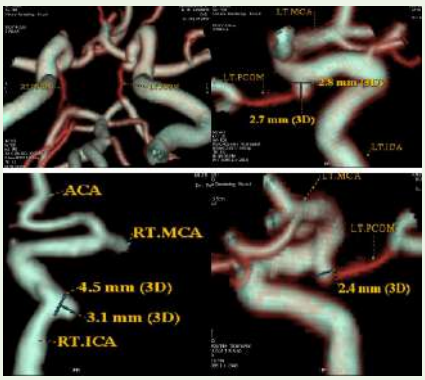

Figure 20: CTCA 3D-VR (A-D) pictures show a right petrous ICA (C2) small saccular aneurysm measuring 3.1x4.5 mm and a left ostio-proximal small PCOM saccular aneurysm measuring 2.7x24 mm with a neck diameter of 2.8 mm. Endovascular therapy was scheduled for him.

Citation: Kumar K, Raveendran C, Murugaiah V, Senthilnathan V. Computed Tomography Cerebral Angiography Evaluation of Cerebral Arterial Aneurysms-Case Series. Indian J Appl Radiol. 2026;12(1): 231.

Case 21: A 61-year-old man who had a history of headaches and vertigo had CTCA.

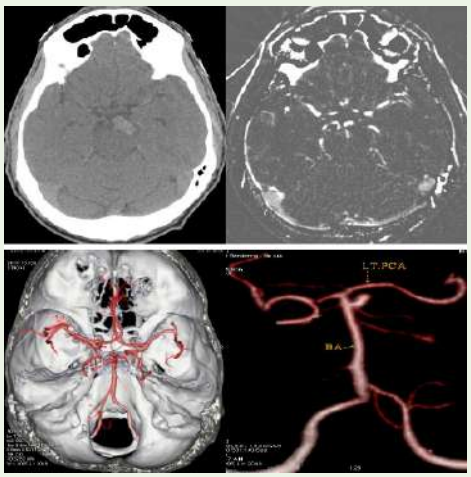

Figure 21: CT Axial non-contrast (A) reveals linear hyperdensity anterior to midbrain on left side, MIP (B), Virtual dissection of skull (C) and 3D -VR (D) images reveal distal basilar artery saccular aneurysm with high ellipticity index projecting to the left side. He was advised endovascular treatment & on interval follow up.

Case 22: 48 years old female with headache not relieved by analgesics sent for CTCA.

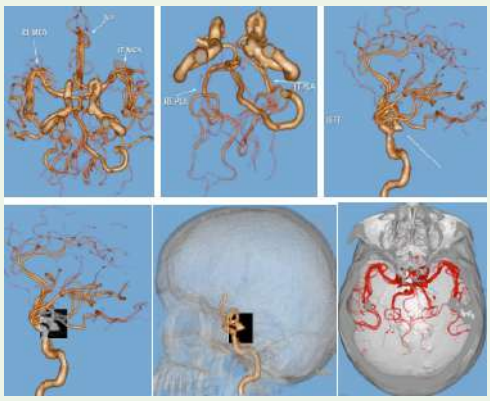

Figure 22: CTCA 3D-VR (A-D) and virtual dissection of the skull (E, F) images show an inferiorly projecting left ostio-proximal PCOM saccular aneurysm. Endovascular therapy and routine follow-up were recommended for her.

Case 23: A 27-year-old male who has a history of severe, recurrent headaches and is known to be an alcoholic was examined using CTCA.

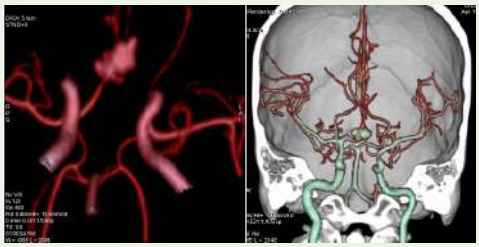

Figure 23: A multilobed medium saccular aneurysm is visible at the intersection of the A1 segment of the right ACA and ACOM in CTCA 3D-VR (A) and virtual bone dissection (B) pictures. Endovascular coiling and/or neurosurgical clipping were recommended for him.

Case 24: A 45-year-old lady receiving treatment for a persistent headache was referred for CTCA.

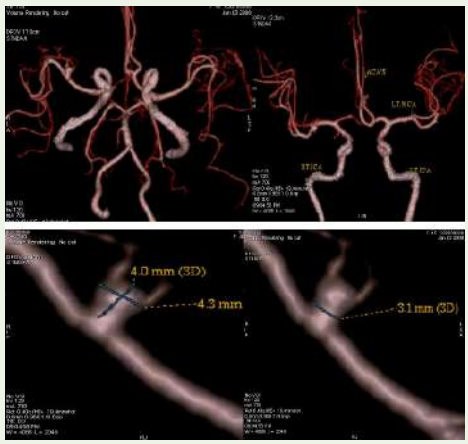

Figure 24: A small saccular aneurysm of the M1 segment of the right MCA, measuring approximately 4x4.3 mm with a neck diameter of 3.1 mm, is visible in CTCA 3D-VR (A-D) pictures. Surgical clipping and/or endovascular coiling were recommended, and she was lost for follow-up.

Case 25: A 38-year-old woman who had dysarthria and a headache underwent CTCA. She had previously experienced uneven therapy for hypertension.

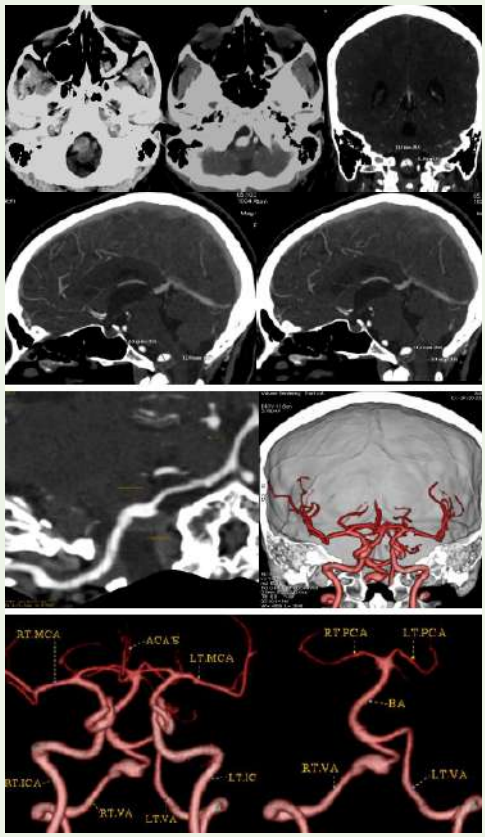

Figure 25: An oval hyperdensity is visible anterior to the medulla in CT axial non-contrast (A). A large right vertebral fusiform aneurysm (Dolichoectasia) measuring 12.8x12.8x11.9 mm with a posterior intramural thrombus measuring 11.1x5.9 mm is visible in axial, coronal, and sagittal contrast images (B-F), virtual dissection (G), and 3D-VR images (H, I). Endovascular therapy and further monitoring were recommended for her.

Citation: Kumar K, Raveendran C, Murugaiah V, Senthilnathan V. Computed Tomography Cerebral Angiography Evaluation of Cerebral Arterial Aneurysms-Case Series. Indian J Appl Radiol. 2026;12(1): 231.

Case 26: A 14-year-old boy who had SAH, received follow-up CTCA after surgery to remove a right ICA bifucation aneurysm.

Figure 26: CTCA 3D-VR images show a surgically clipped right ICA bifurcation aneurysm.

Microaneurysms, also called Charcot-Bouchard aneurysms, are linked to persistent hypertension and usually develop in small blood arteries (less than 300 micrometers in diameter), most frequently the lenticulo-striate vessels of the basal ganglia [8]. Intracranial bleeding is frequently caused by Charcot-Bouchard aneurysms [9].

A family history of aneurysms, a variety of hereditary illnesses, age above 50, female gender, present cigarette smoking, and cocaine usage are all contributing factors to the development of aneurysms. Rare causes of intracranial aneurysms include head trauma, intracranial tumors or neoplastic emboli, and infections from bacterial or fungal colonization of artery walls [10].

Intracranial aneurysms have been linked to fibromuscular dysplasia, coarctation of the aorta, and pheochromocytoma, most likely due to the elevated blood pressure that these disorders induce [11].

SAH is 1.6 times more prevalent in women, making them more vulnerable to aneurysm rupture [12-14]. Only 10–15% of cerebral aneurysms exhibit symptoms [15, 16], with the majority being discovered by chance while being evaluated for other ailments. The bulk effect or possibly a little amount of blood leakage that irritates the meninges but is insufficient to qualify as a hemorrhage are the main causes of the CAA symptoms [12, 17]. Given that 10% to 43% of SAH sufferers report having a sentinel headache two months prior, these symptoms could be an early warning sign of an imminent rupture.preceding the rupture [18]. SAH patients typically have poor clinical conditions, which might include severe headaches, disorientation, neurological impairments, and even coma. With a 25% to 50% death rate, SAH is a terrible occurrence. Only about one-third of cases have a favorable outcome since over 50% of survivors experience permanent impairment [19].

According to statistics from the International Study of Unruptured Intracranial Aneurysms (ISUIA), aneurysms with a diameter of 10 mm or greater are critically vulnerable to rupture. The average annual rupture rate for aneurysms smaller than 10 mm in diameter without a history of SAH was 0.05%; however, the rupture rate was ten times higher for aneurysms of the same size with a history of SAH [20].

For the detection of cerebral aneurysms, a recent study using CTCA with a multidetector row scanner found a sensitivity of 95.1% to 98% and a specificity of 100%. The published series shown that DSA is still more sensitive than CTCA in detecting aneurysms less than 3 mm [21, 22]. In addition to screening, CTCA may identify the morphometric features of intracranial aneurysms, such as the sizes of the sac and neck as well as the existence of daughter sacs and leaving branches. An ECG-gated, time-resolved, volumetric imaging sequence, four-dimensional (4D) CTCA generates angiographic images using patient-specific average input rates with a rather excellent spatial resolution (≈0.5 mm^3) [23]. The method is being applied more frequently to improve hemodynamic assessments of brain aneurysms using computational fluid dynamics (CFD). 4D CTCA has been shown in several investigations to detect specific regions of abnormal aneurysm wall motion, which may indicate a higher risk of rupture [24]. For cerebral aneurysms greater than 3 mm, the three-dimensional (3D) time-of-flight (TOF) MRA sensitivity is 93%–97%, while for aneurysms smaller than 3 mm, it is 85%-93% [25].

To see cerebral arteries and their aneurysms, 4D MR employs gadolinium contrast and TOF sequences. 4D MR uses post-processing techniques and ECG-synchronized 3-D phase-contrast MRI to noninvasively measure 3-D intracranial blood flow [26]. In specific regions of interest, 4D MR may evaluate blood flow volumes, flow velocities, and wall shear stress (WSS). A number of modest investigations have shown that aberrant WSS may be linked to thin aneurysm walls and aneurysm development [27], which could have therapeutic implications.

Research indicates that an inflammatory mechanism that results in artery wall remodeling, atherosclerotic conformation, and aneurysm growth is the cause of aneurysms [28]. Focal enhancement aneurysms are more likely to be bigger [28] and have a higher rupture risk score [29].

When evaluating unstable unruptured intracranial aneurysms, MR high-resolution vascular wall imaging (HR-VWI) has emerged as a valuable tool. The evaluation of aneurysm wall enhancement as a biomarker of aneurysm wall inflammation, aneurysm growth, and rupture shows encouraging compliance [30]. According to data, there is a significant negative predictive value for the absence of aneurysm wall augmentation. When there are several intracranial aneurysms, MR HR-VWI can assist in identifying the ruptured aneurysm and may even lead to rupture risk classification during aneurysm surveillance [31].

With 3D rotating DSA, the operator may see the aneurysm's size, shape, and neck as well as the parent-vessel properties in more detail. Additionally, this method is helpful in obtaining suitable working angles for potential endovascular expected anatomy and embolization following open surgical surgery [32, 33]. With the exception of vascular overlap, 4D DSA allows 3D viewing from any chosen spatial projection at any moment throughout the passage of the contrast bolus for aneurysm investigation [34].

Due to early IVUS catheters' enormous size and poor navigability, intravascular ultrasonography (IVUS) has been limited in its ability to evaluate cerebral disease. Furthermore, IVUS is known to overestimate the true lumen's size, which could be caused by inadequate lumen–intima interface imaging [35].

An alternative intravascular imaging method called optical coherence tomography (OCT) employs interferometry and light

Citation: Kumar K, Raveendran C, Murugaiah V, Senthilnathan V. Computed Tomography Cerebral Angiography Evaluation of Cerebral Arterial Aneurysms-Case Series. Indian J Appl Radiol. 2026;12(1): 231.

Table 1: List of cases

Case no	Age	Sex	Clinical presentation	Aneurysm location	Size	Morphology
1	70	Female	Intense headache, eye pain, right side weakness, numbness. Hypertension. SAH	Left MCA bifurcation	Medium	Saccular
2	60	Female	Persistent headache, meningeal signs, neurological impairement. Hypertension. Type 2 diabetes. SAH	Right MCA bifurcation	Medium Dome- 9.5x6mm Neck- 3.5mm	Saccular multilobed
3	65	Female	Seizures, loss of consciousness, Hypertension. SAH, IVH	ACOM	Small Neck -3.7 mm	Saccular
4	48	Male	Severe headache, chronic smoker. SAH	1.ACOM 2. Left MCA bifucation	Medium Dome- 10.8x7.6 mm. Small Dome-6.1x4.9 mm	Saccular multilobed Saccular
5	62	Male	Severe headache, nausea, vomiting, Hypertension. SAH	1.Left Clinoid ICA (C5) 2.ACOM 3.Right MCA 4. Left PCA	Small Small Small Small	Saccular Saccular sacculaS Fusiform
6	50	Male	Severe thunderclap headache, left double vision, alcoholic. SAH	Left ICA (C4)	Small	Saccular
7	63	Male	Severe headache, Hypertension SAH	ACOM	Medium Neck-3.4 mm	Saccular
8	70	Male	Left hemiperesis, Altered sensorium, Hypertension, Type 2 Diabetes, right frontal lobe lobulated hematoma, SAH, IVH	Right ACA (A3)	Large	Saccular
9	65	Male	Left focal neurological impairment, impaired sensorium. Right temporal lobe lobulated hematoma	Right MCA (M1)	Small	Saccular
10	43	Female	Left leg sensory loss & weakness. Right frontal lobe infarct	ACOM	Large	Saccular
11	63	Male	Persistent headache, smoker	ACOM	Small	Saccular
12	75	Male	Recurrent headache, Hypertension	1. ACOM 2. Bilateral ACA (A2)	Large Small	Saccular Saccular
13	50	Male	Persistent headache,	1. Left ICA bifurcation 2. Left MCA bifurcation	Large Dome-10.2x9.4mm Neck-7.1mm Small Dome-3.2x2.9mm	Saccular multilobed with bleb Saccular
14	65	Female	Frequent headache, Type 2 diabetes milletus	Right ICA bifurcation & origin of PCOM	Medium Neck -4mm	Saccular
15	60	Female	Persistent, recurrent headache	1. Right ICA bifurcation 2. Intersection of right PCOM & MCA	Small Dome-5 x 4.1 mm. Neck -4.7 mm Medium Dome-9.5x9mm Neck-5mm	Saccular Saccular multilobed
16	62	Male	Frequent headache Hypertension	Right distal communicating ICA (C7)	Medium Neck-2.4 mm & 2mm	Saccular
17	55	Female	Persistent headache Previous SAH	1.Left ICA bifurcation 2.Left terminal communicaating ICA (C7)	Large Small Neck-3.7mm, 3.6 mm, and 2.2 mm	Saccular Saccular
18	64	Male	Persistent headache Left eye blurred vision	Left ophthalmicICA (C6)	Small	Saccular
19	45	Male	Bilateral impaired vision, persistent, severe headache	Bilateral ophthalmicICA (C6)	Right medium Dome- 9.6x5.9 mm Neck -4.5 mm Left small Dome- 3.3x3.4 mm Neck -3.9 mm	Saccular

Citation: Kumar K, Raveendran C, Murugaiah V, Senthilnathan V. Computed Tomography Cerebral Angiography Evaluation of Cerebral Arterial Aneurysms-Case Series. Indian J Appl Radiol. 2026;12(1): 231.

20	35	Male	Persistent headache	1. Right petrous ICA (C2) 2. Ostio-proximal Left PCOM	Small Dome- 3.1x4.5 mm Dome-2.7x24 mm Neck -2.8 mm.	Saccular
21	61	Male	Headache, vertigo	Basilar atery, distal	Medium Neck -2.2mm	Saccular
22	48	Female	Headache	Left ostio-proximal PCOM	Small	Saccular
23	27	Male	Severe recurrent headache, alcoholic	Intersection of A1 segment of right ACA and ACOM	Medium	Saccular multilobed
24	45	Female	Persistent headache	M1 segment of Right MCA. Dome- 4x4.3 mm, Neck - 3.1 mm	Small	Saccular
25	38	Female	Dysarthria, Headache, Hypertension	Right vertebral	Large 12.8x12.8x11.9 mm with posterior intramural thrombus measuring 11.1x5.9mm	Fusiform (Dolichoectasia)
26	14	Male	SAH	Operated Right ICA bifurcation. Surgical clip	Medium	Saccular

backscatter to see the architecture of the artery wall and lumen with a spatial resolution ten times greater than that of DSA or IVUS [36]. OCT can scan lumen size, intimal flaps, patency of perforators and tiny branches, stent apposition, thrombus development, endothelialization, and all layers of the artery wall with an axial resolution of 10 to 20 μm, which may be useful in predicting aneurysm rupture [37].

The 2D and 3D morphology of aneurysms can be evaluated in a variety of ways, such as aneurysm width, perpendicular height, maximum height (from the midpoint of the neck), numerous lobes, blebs, aneurysm angle, aneurysm volume, neck width aspect ratio (height divided by neck width), and parent-vessel diameter size ratio (maximum diameter to parent-vessel diameter) [38].

The following suggestions are included in the American Heart Association [39] consensus guidelines for the standardized reporting on imaging for intracranial aneurysms and endovascular repair:

1. When there are several aneurysms, each one needs to be explained separately.

2. High-resolution planar reconstructed images are used to provide aneurysm dome measures in millimeters in three orthogonal planes. To prevent attenuating the precise lumen size and morphology, the source images shouldn't be over-windowed.

3. The location of the aneurysm is described on the base of the neck origin vessel and, often, the nearest branchship. For example, the closest branch vessel, such as the meningo-hypophyseal trunk, superior hypophyseal, ophthalmic, anterior choroidal, or posterior communicating artery, or position at the carotid terminus, should be used to name ICA aneurysms. Bony landmarks, such as the supraclinoid, should not be used for description since they are less accurate.

4. Although additional coordinate planes (anterior or posterior, superior or inferior, medial or lateral) are also frequently used, aneurysm orientation can be characterized as right of midline, midline, or left of midline. It is also necessary to discuss the impacts of mass on nearby structures.

5. Neck sizes smaller than 4 mm and aneurysm dome-to-neck ratios larger than 2:1 indicate aneurysm morphology that can be coiled. The neck's dimensions in comparison to the parent vessel diameter is also an important determinant for use of intraluminal adjunctive devices or flow diverters.

When using flow diverters or intraluminal adjunctive devices, vessel diameter is another crucial factor. The best way to visualize complex aneurysm morphology is via 3D volume-rendering software.

The three management approaches are surgical clipping, endovascular coiling, and observation (Figure 26). Fusiform aneurysms are currently treated using a variety of techniques, including bypasses, vascular stents, wrapping, and trapping. Treatment for cerebral aneurysms is becoming safer and more efficient thanks to nonoperative endovascular methods. It is debatable what should be done when cerebral aneurysms remain unruptured.

The initial interval imaging is typically obtained after three to six months of treatment, since most aneurysm recurrences happen in the first year after treatment [40]. The subsequent picture is taken between six months and a year later if it is stable at that point. Imaging may be stretched out to intervals of one to five years if the aneurysm continues to show stability. Higher-threat aneurysms require a longer (perhaps lifetime) follow-up period [41].

The gold standard for vascular imaging, DSA is typically chosen for the first follow-up imaging following aneurysm therapy. For long-term surveillance, MRA is the preferred noninvasive imaging technique. Since gadolinium contrast carries a relatively low risk [39], CE-MRA is typically chosen. The acquisition duration is quicker than TOF-MRA, and TOF-MRA is less sensitive for aneurysms that perfuse slowly [42]. Because there is less susceptibility artifact associated with stents and flow diverters with high metal surface coverage and flow-related signal loss is eliminated by the use of contrast material, the CE-MRA exhibits better detection of post-treatment intracranial aneurysm occlusion, parent vessel visualization, and luminal measurements even though its inherent spatial resolution is lower than that of the 3D TOF technique [43].

Although CTCA is an inexpensive, noninvasive substitute for

Citation: Kumar K, Raveendran C, Murugaiah V, Senthilnathan V. Computed Tomography Cerebral Angiography Evaluation of Cerebral Arterial Aneurysms-Case Series. Indian J Appl Radiol. 2026;12(1): 231.

MRI, beam hardening artifacts from clips, coils, and stents severely impair the image quality [44].

Conclusion

The diagnosis, monitoring, therapy, and post-treatment monitoring of cerebral aneurysms all depend on imaging. In order to more precisely guide implicit treatment, it is crucial to accurately assess the size, morphology, position, and rupture status of a cerebral aneurysm as well as to identify certain imaging characteristics that may indicate a higher risk of rupture. The majority of intracranial aneurysm morphologies may be accurately and noninvasively diagnosed by radiologists using CTCA quickly in emergency room setting, which is necessary to select the best course of action. Therefore, it seems that employing CTCA as the main imaging technique for SAH is a successful strategy, and DSA should only be used in situations when there is doubt. Non-invasive imaging techniques like as transcranial Doppler sonography, CTCA, and MRA are more suitable for serially monitoring aneurysms because of invasive angiography's risks. Treatment for cerebral aneurysms is becoming safer and more efficient thanks to nonoperative endovascular procedures.

References

1. Greving JP, Wermer MJH, Brown RD Jr, Morita A, Juvela S, et al.(2014) Development of the PHASES score for prediction of risk of rupture of intracranial aneurysms: a pooled analysis of six prospective cohort studies. Lancet Neurol 13: 59-66.
2. Brisman JL, Song JK, Newell DW (2006) Cerebral aneurysms. N Engl J Med 355: 928-939.
3. Sanei Taheri M, Haghightkhah HR, Noori M (2009) A Pictorial Essay on Uncommon Patterns of Intracranial Aneurysms. Iran Journal of Radiol 6: 237-246.
4. Howlett D, Ayers B (2004) The hands-on guide to imaging. Oxford: Blackwell Pp: 204.
5. Hemorrhage S (1998) In: Ellison D, Love S. Neuropathology: a reference text of CNS pathology. St. Louis: Mosby 1998:10.3-10.8.
6. Morita A, Kirino T, Hashi K, Aoki N, Fukuhara S, Hashimoto N, et al. (2012) The natural course of unruptured cerebral aneurysms in a Japanese cohort. N Engl J Med, 366: 2474-2482.
7. Sarica FB, Cekinmez M, Tufan K, Sen O, Erdogan B, et al. (2008) A non-bleeding complex intracerebral giant aneurysm case: case report. Turk Neurosurg 18: 236-240.
8. Kumar V, Abbas A, Fausto N, (2005) Robbins and Cotran Pathologic Basis of Disease (7th ed.). China: Elsevier.
9. Gupta K, Das MJ (2021) Charcot Bouchard Aneurysm, Treasure Island (FL): StatPearls Publishing, PMID 31971704, retrieved 2021-05-06.
10. Charles Vega, Jeremiah V. Kwoon, and Sean D (2002) Lavine, Intracranial Aneurysms: Current Evidence and Clinical Practice. American Family Physician. 66: 601-608.
11. Wardlaw J M, White P M (2000)The detection and management of unruptured intracranial aneurysms. Brain 123: 205-221.
12. Gasparotti R, Liserre R (2005) Intracranial aneurysms. Eur Radiol 15: 441-447.
13. Wardlaw JM, White PM (2000) The detection and management of unruptured intracranial aneurysms. Brain 123: 205-221.
14. Wagner M, Stenger K (2005) Unruptured intracranial aneurysms: using evidence and outcomes to guide patient teaching. Crit Care Nurs Q 28: 341-354.
15. Friedman JA, Piepgras DG, Pichelmann MA, Hansen KK, Brown RD Jr, ET AL. (2001) Small cerebral aneurysms presenting with symptoms other than rupture. Neurology 2001; 57: 1212-1216.
16. Wiebers DO, Whisnant JP, Huston J 3rd, Meissner I, Brown RD Jr, Piepgras DG et al. (2003) Unruptured intracranial aneurysms: natural history, clinical outcome, and risks of surgical and endovascular treatment. Lancet 362:103-110.
17. Rowley HA (2007) Cerebrovascular disease. In: Brant W, Helms C, editors. Fundamentals of diagnostic radiology. Philadelphia: Williams and Wilkins; Pp: 86-122.
18. Polmear A (2003) Sentinel headaches in aneurysmal subarachnoid haemorrhage: what is the true incidence? A systematic review. Cephalalgia 23: 935-941.
19. Wardlaw JM, White PM (2000)The detection and management of unruptured intracranial aneurysms. Brain 123: 205-221.
20. Unruptured intracranial aneurysms-risk of rupture and risks of surgical intervention. International Study of Unruptured Intracranial Aneurysms Investigators. N Engl J Med 1998;339: 1725-1733.
21. Agid R, Lee SK, Willinsky R, Farb RI, terBrugge KG, et al. (2006) Acute subarachnoid hemorrhage: using 64-slice multidetector CT angiography to "triage" patients' treatment. Neuroradiology 48: 787-794.
22. Yoon DY, Lim KJ, Choi CS, Cho BM, Oh, SM, et al. (2007) Detection and characterization of intracranial aneurysms with 16-channel multidetector row CT angiography: a prospective comparison of volume-rendered images and digital subtraction angiography. AJNR Am J Neuroradiol 28: 60-67.
23. Biswas S, Chandran A, Radon M, Puthuran M, Bhojak M, et al. (2015) Accuracy of four-dimensional CT angiography in detection and characterisation of arteriovenous malformations and dural arteriovenous fistulas. Neuroradiol J 28: 376-384.
24. Zhang J, Li X, Zhao B, Zhang J, Sun B, et al. (2021) Irregular pulsation of intracranial unruptured aneurysm detected by four-dimensional CT angiography is associated with increased estimated rupture risk and conventional risk factors. J Neurointerv Surg. 13:854-859.
25. Kapsalaki EZ, Rountas CD, Fountas KN (2012) The Role of 3 Tesla MRA in the Detection of Intracranial Aneurysms. Int J Vasc Med 2012: 792834.
26. Markl M, Chan FP, Alley MT, Wedding KL, Draney MT, et al. (2003) Time-resolved three-dimensional phase-contrast MRI. J Magn Reson Imaging 17: 499-506.
27. Van Ooij P, Potters WV, Guédon A, Schneiders JJ, Marquering HA, et al. (2013) Wall shear stress estimated with phase contrast MRI in an in vitro and in vivo intracranial aneurysm. J Magn Reson Imaging 38: 876-884.
28. Lv N, Karmonik C, Chen S,Wang X, Fang Y, et al. (2019) Relationship Between Aneurysm Wall Enhancement in Vessel Wall Magnetic Resonance Imaging and Rupture Risk of Unruptured Intracranial Aneurysms. Neurosurgery 84: E385–E391.
29. Hartman JB, Watase H, Sun J, Hippe DS, kim L, et al. (2019) Intracranial aneurysms at higher clinical risk for rupture demonstrate increased wall enhancement and thinning on multicontrast 3D vessel wall MRI. Br J Radiol 92: 20180950.
30. Texakalidis P, Hilditch CA, Lehman v, Lanzino G, Pereira VM, et al. (2018) vessel wall imaging of intracranial aneurysms: systematic review and meta-analysis. World Neurosurg 117: 453-458.
31. Santarosa C, Cord B, Koo A, Bhogal P, Malhotra A, et al. (2020) Vessel wall magnetic resonance imaging in intracranial aneurysms: Principles and emerging clinical applications. Interv Neuroradiol 26:135-146.
32. van Rooij WJ, Sprengers M, deGast AN, PelusoJ, Sluzewski M (2008) 3Drotational angiography: the new gold standard in the detection of additional intracranial aneurysms. Am J Neuroradiol 29: 976-979.
33. Wong SC, Nawawi O, Ramli N, Abd Kadir KA (2012) Benefits of 3D rotational

Citation: Kumar K, Raveendran C, Murugaiah V, Senthilnathan V. Computed Tomography Cerebral Angiography Evaluation of Cerebral Arterial Aneurysms-Case Series. Indian J Appl Radiol. 2026;12(1): 231.

DSA compared with 2D DSA in the evaluation of intracranial aneurysm. Acad Radiol 19: 701-707.

34. Sandoval-Garcia C, Royalty K, Yang P, Niemann D, Ahmed A, et al. (2016) 4D DSA a new technique for arteriovenous malformation evaluation: a feasibility study. J Neurointerv Surg 8: 300-330.

35. Kubo T, Akasaka T, Shite J, Suzuki T, Uemura S, et al. (2013) OCT compared with IVUS in a coronary lesion assessment: the OPUS-CLASS study. JACC Cardio vasc Imaging 6: 1095-1104.

36. Chen CJ, Kumar JS, Chen SH, Ding D, Buell TJ, et al. (2018) Optical coherence tomography: future applications in cerebrovascular imaging. Stroke 49: 1044-1050.

37. Anagnostakou V, Ughi GJ, Puri AS, Gounis MJ (2021) Optical coherence tomography for neurovascular disorders. Neuroscience. 474: 134144.

38. Beaman C, Patel SD, Nael K, Colby GP, Liebeskind DS (2023) Imaging of Intracranial Saccular Aneurysms Stroke Vasc Interv Neurol 3: e000757.

39. Meyers PM, Schumacher HC, Higashida RT, Derdeyn CP, Nesbit GM, et al. (2009) Reporting standards for endovascular repair of saccular intracranial cerebral aneurysms. Stroke 40: e366-e379.

40. Campi A, Ramzi N, Molyneux AJ, Summers PE, Kerr RS, et al. (2007) Retreatment of ruptured cerebral aneurysms in patients randomized by coiling or clipping in the International Subarachnoid Aneurysm Trial (ISAT). Stroke 38: 1538-1544.

41. Prince MR, Zhang H, Zou Z, Staron RB, Brill PW (2011) Incidence of immediate gadolinium contrast media reactions. AJR Am J Roentgenol 196: W138-W143.

42. Serafin Z, Strze´sniewski P, Lasek W, BeuthW (2011) Methodsandtimeschedule for follow-up of intracranial aneurysms treated with endovascular embolization: a systematic review. Neurol Neurochir Pol 45: 421430.

43. Boddu SR, Tong FC, Dehkharghani S, Dion JE, Saindane AM (2014) Contrast-enhanced time-resolved MRA for follow-up of intracranial aneurysms treated with the pipeline embolization device. AJNR Am J Neuroradiol 35: 2112-2118.

44. Soize S, Gawlitza M, Raoult H, Pierot L (2016) Imaging follow-up of intracranial aneurysms treated by endovascular means: why, when, and how? Stroke 47: 1407-1412.

Citation: Kumar K, Raveendran C, Murugaiah V, Senthilnathan V. Computed Tomography Cerebral Angiography Evaluation of Cerebral Arterial Aneurysms-Case Series. Indian J Appl Radiol. 2026;12(1): 231.